Performance Assessment of Thermal Bridge Elements into a Full Scale Experimental Study of a Building Façade

Roberto Garay, Amaia Uriarte, Inés Apraiz

Tecnalia, Sustainable Construction Division
Parque Tecnológico de Bizkaia, C/ Geldo, Edificio 700
48160 – Derio, Spain
Roberto.Garay@tecnalia.com

In this paper, an experimental and numerical approach to the characterization of thermal bridges is presented. The need for this characterization was found within an experimental study in a 2 floor high façade. This façade was constructed with 3 concrete elements which were placed in it to produce a similar thermal bridge effect to the one created by floor slabs traditional building construction in Spain.

Commonly applied thermal assessments perform one-dimensional heat transfer analysis over planar elements such as the façades studied in this experiment. However, it is well known that thermal bridges are locations in buildings where one-dimensional heat transfer analysis can not be applied.

This problem was approached by creating a numerical 2D thermal model which was calibrated against experimental data from several temperature and heat flux sensors which were locate at specific points in the thermal bridge elements.

1. Introduction

Building energy consumption sums up to 40% of primary energy consumption in developed countries [1] [2] [3] [4] . Aside from energy needs for appliances or Domestic Hot Water, a large amount of this is required for space heating and cooling, to meet occupants comfort requirements. Intensive studies and development of techniques for the assessment of heating, cooling and air conditioning energy consumption of buildings have been conducted during more than 50 years. Testing and calculation methods have been developed, ranging from standardized material testing procedures to dynamic simulation software tools [5] .

Heat transfer through building envelopes is one of the main terms in the heat balance of buildings, and special attention is paid on them to ensure a proper thermal insulation level.

In the last half of the past century, building energy codes have forced a trend towards more insulated building envelopes. This trend has been boosted by EU Energy Performance of Buildings Directives (EPBD) [3] [4] , adopted by all EU member states. In this context, the relative relevance of thermal bridges has grown.

Furthermore, in developed countries in Europe, the ageing building stock is involved into a thermal performance upgrade under the previously mentioned EPBD policies. Building envelope upgrade processes are being conducted with systems such as External Thermal Insulation Systems (ETHICS). These systems potentially allow for a nearly complete avoidance of certain thermal bridges, but their practical implementation leads to performance uncertainties.

A detailed analysis on the relevance of thermal bridges and how building codes deal with them in EU Member States was performed in [6] . The relevance of thermal bridges in the energy assessment of buildings was estimated in upto 30% of heating

energy demand. This being more relevant within highly insulated buildings. It was identified that although all building codes considered thermal bridges, these were commonly assessed through conservative default values. When dealing with renovation projects for already built buildings, the energy requirements for junctions are reduced or even not-imposed. The use of improved junctions compared to national default values was evaluated at 15 %.

In this context, an experiment was carried out in order to assess the thermal performance improvement of one of such façade refurbishment methods.

This experiment was conducted in the Kubik by tecnalia research facility [7] [8] . This is a research infrastructure located in Derio, Spain, focused on full scale testing of energy efficiency within the building sector. Its main goal being to bridge the gap between laboratory testing and full scale market deployment of building envelopes, HVAC & ICT solutions for Energy Efficiency, where the full energy interaction between different elements is evaluated.

Fig 1 Kubik by tecnalia research facility. General view (left) & specific façade used for the experiment (right)

A 2 storey- high façade was constructed in the Kubik by Tecnalia test facility and several thermal bridge elements were located in it. However, due to the need to assess heat transfer through these elements, a multidimensional heat transfer model was created and calibrated.

Building envelopes are mainly characterized by one-dimensional (1D) heat transfer formulae are applied, neglecting the effect of hetereogenous elements (beams, window sills…). However, thermal bridges are common in places where structural stresses are transmitted from façades to beam elements, or where different kinds of envelope constructions meet, etc. with variations in the geometry & materials among the different sides of the joint. In these areas, bi- or tri-dimensional (2D /3D) heat transfer phenomena is present, and 1D assumptions can not be applied.

3D heat transfer accounts for a small share of the total heat transfer in a building, as it is restricted to corners. However, although not addressed in this paper, 3D thermal bridges are common locations for cold spots where condensation and mold growth can occur.

In common practice, building envelope heat transfer is commonly approached as 1D heat flow over the full envelope surface, considering an additional linear heat transfer, related to the length of the edge in which 2D heat flows occur, as formulated in Eq 1.

$$\psi = L^{2D} - \sum U_j * l_j$$

Eq 1 Linear Transmitance according to [9]

Performance values of envelope constructions are most commonly provided through steady state approaches under standardized procedures: [10] for 1D & [11] [12] for 2D/3D heat transfer.

However, this approach lacks precision when the dynamic behavior of a full building/room needs to be evaluated. In most building energy simulation (BES) software, only 1D heat flow is calculated under dynamic boundary conditions. 2D/3D heat flow being incorporated as an increased value of 1D heat transfer, calculated under various simplifying approaches. Methods to implement dynamic 2D/3D heat flow into BES software have already been developed. In [13] , a method for introducing dynamic 2D heat transfer in energy plus is developed, while in [14] [15] [16] [17] , a transfer

function of a 2D thermal bridge is obtained both through finite element & experimental techniques.

In the framework of the already mentioned testing of different façades under external weather exposure and internal dynamic conditions, such a dynamic 2D heat transfer method was required. This paper providing the procedure for the experimental calibration of 2D Finite Difference Model (FDM), used for the obtention of the dynamic heat transfer of the thermal bridge. This process involved the location of several sensor devices in the elements themselves, the construction of the 2D FDM, and the calibration of the models to meet experimental results.

However, as FDMs only accounted for a small fraction of the total geometry of the test cells, results coming from this FDM needed to be coupled with measured data from 1D heat transfer areas and HVAC systems.

In this framework, the results from the FDM were processed to convert them into a dynamic linear heat transfer transmittance, as it is further developed in chapter 8.

This process was found necessary not only because of its influence in the accuracy of the heat balance of the test cells, but also because one of the foreseen results was the thermal performance improvement of these elements, over the sequence of tested façades. This required of this experimental/numerical process being established to assess this improvement.

2. Process

The identification of 2D heat transfer through beam elements in façades was performed in a process which involved several steps.

- Definition of the mathematical integration frame for the assessment of the thermal bridges. (Section 3)
- Identification of suitable places for sensor placement (Section 5)
- Installation of sensors
- Experimental campaign (Section 6)
- 2D FDM modeling and calibration (Section 7)
- Integration of the calibrated models into the main room model (Section 10)

3. Integration Frame

Within a research project for the assessment of thermal improvement of building fabric through façade refurbishment, an experiment was conducted in which heat transfer through a building envelope was experimentally obtained.

This experiment was conducted in the Kubik by tecnalia research facility, where a sub-sector consisting of two test-rooms in a vertical arrangement were conditioned for this test. A west-oriented test façade was constructed in these rooms, which comprised 3 beam elements, constructed in equivalent materials and thicknesses to those present in the Spanish building stock.

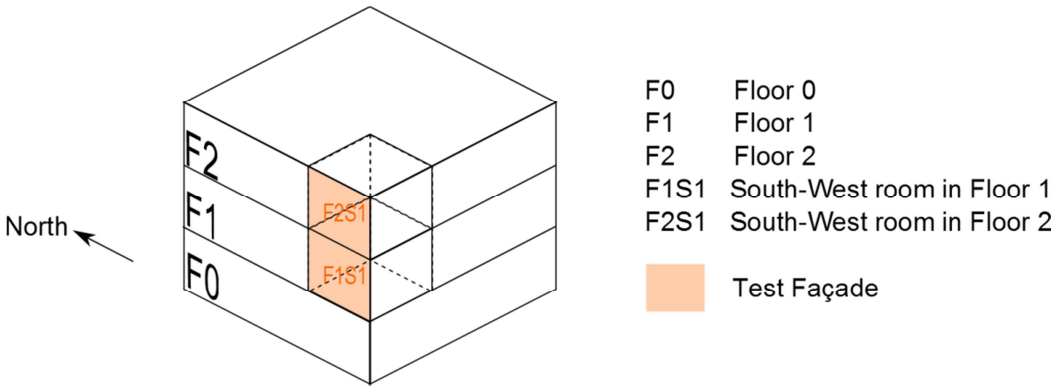

Fig 2 Scheme of test rooms

These 3 beam elements were located at slab level coincident with 1st, 2nd and roof level slabs in Kubik. All 3 elements were kept constant in the experiment, while a sequence of façades was experimented.

Thermal bridges in all 2D & 3D details were modeled in steady-state conditions during the architectural design of this test, and these results used to generate roubst constructions details. These details achieved the goal of reducing relevant energy flows to only 1D and 2D heat transfer through concrete.

The experimental campaign was developed in three phases, where different façade constructions were placed in the same façade:

- Phase 0: Highly insulated sandwich façade
    - 20cm PU sandwich façade
    - Additional 10cm XPS placed internally
- Phase 1: Brick cavity façade
    - Internal brick wall: Mortar (1,5cm aprox) rendered hollow brick (7cm)
    - Cavity: 10cm air gap
    - External brick wall: 11cm perforated brick
- Phase 2: Ventilated façade refurbishment of brick cavity façade
    - Tiles: 1cm ceramic tiles
    - Cavity: 5cm, ventilated
    - Insulation: 5cm Mineral wool
    - Base wall: Pre-existing from Phase 1.

The configuration of each phase is shown in Fig 3

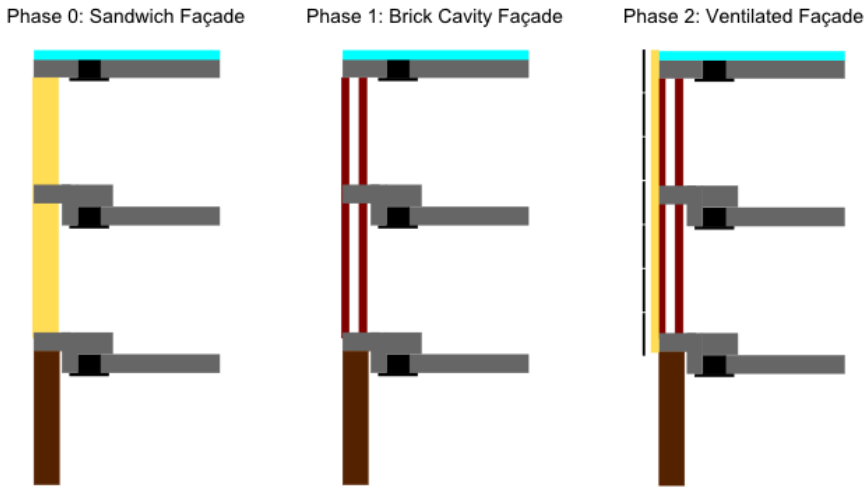

Fig 3 Vertical section of the west façade layout, for all experimental phases

In all three phases, the effect of the building fabric within the thermal balance of the building was experimentally evaluated. The heat balance of each test-room was formulated as shown in Eq 2.

$$0 = Q_{HVAC} + \sum_{1D} Q_{1D} + \sum_{2d} Q_{2D} + C$$

Eq 2 Heat balance of a test room

Where:

- Q_{HVAC} represented the thermal output of the HVAC system
- $\sum_{1D} Q_{1D}$ represented the one-dimensional heat transfer through the building fabric
- $\sum_{2d} Q_{2D}$ represented the incremental two-dimensional heat transfer through the building fabric by the beam elements. All 2D heat transfer is neglected except that occurring through the beam elements.
- C represented an uncertainty value which also comprised all the non-considered heat flows.

This balance was formulated and solved for each of the test cells, considering the air volume enclosed in them as “well-mixed”. This approach was considered consistent as the HVAC system consisted on a fan coil system which provided a good air circulation in the test rooms.

The heat balance of the test cell was formulated in a dynamic way and solved for every considered time step (every hour). The heat balance is formulated over the enclosed air volume, whose thermal storage was neglected, the heat capacity and the oscillation of the temperature of this fluid being low, especially when compared with the heat transfer over the enclosing surfaces.

Although several definitions of 1D and 2D heat flows are available, within this project the following definition was applied:

- Control volumes of test rooms were approached as hexahedral volumes limited by the internal surfaces of building elements.

- 1D heat flows were measured in clearly 1D heat flow zones and applied over the full corresponding surface of the test-room model.
- The additional heat flow generated by 2D heat flows in beam elements was calculated and introduced in the test-room model as a linear heat transfer in the corresponding edge.
- Convective and radiative heat exchange of the façade are jointly considered as a surface/boundary heat exchange.

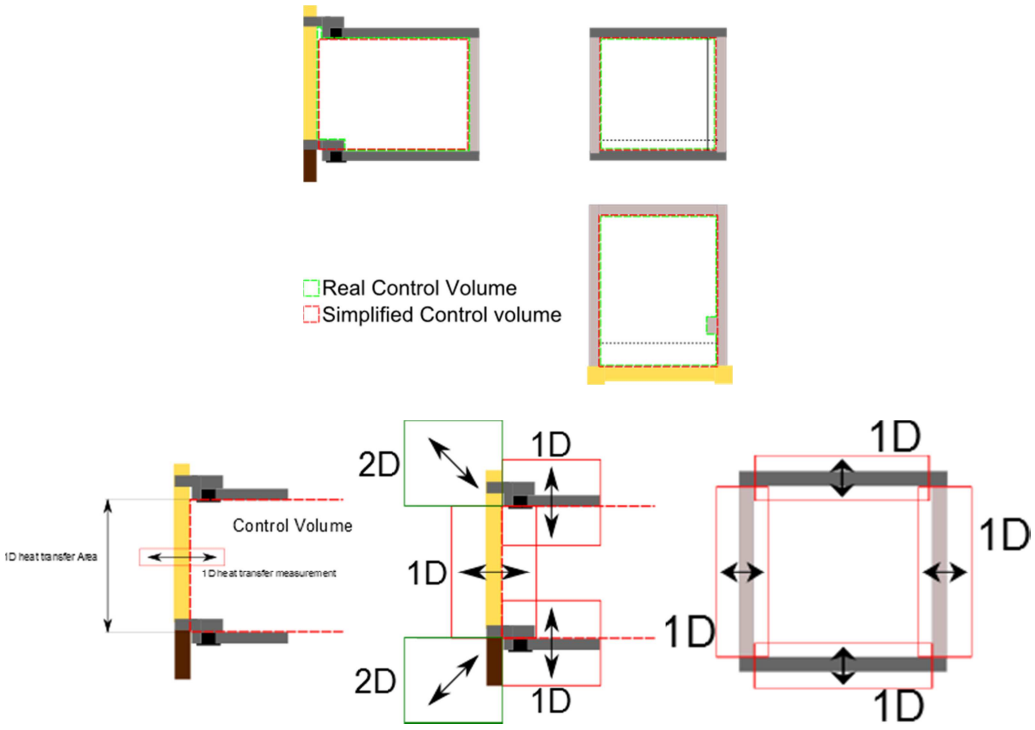

Fig 4 Definition of Control volume (Upper); Definition of 1D heat transfer measurement and application area (Lower left); 1D/2D heat transfer zones in the thermal model of the west façade (Lower centre); Simplified 1D model of non-façade areas (Lower right)

The calculation of the additional 2D heat flow was calculated through a calibrated 2D FDM model. A measurement, modeling and calibration process was performed on each of these particular construction details, which is described in the following chapters.

The uncertainty value (C in Eq 2) is the only unknown value in Eq 2 as the other three heat flows are measured (Q_{HVAC} and $\sum_{1D} Q_{1D}$) or obtained through the calibrated model ($\sum_{2d} Q_{2D}$) which is developed in this paper. So the C value can be obtained by the application of Eq 2 and serve as a dynamic (time dependant) indicator of the uncertainty due to non-measured or modeled phenomena.

4. Joint surface Convective & Radiative heat transfer approach for internal surfaces

Internal heat transfer coefficients are identified from experimental data in the calibration process of the 2D FDM.

It is well known that wall surfaces exchange heat with their surrounding environment through convection and radiation processes. Roughly defined, convection is related with the temperature of the surrounding air, while radiation is related with the average radiant temperature of the surfaces enclosing this environment. In the case of rooms or test cells, this average radiant temperature is related to the temperature of wall/slab surfaces and the surface-to- surface view factor. In the case of external conditions, this is related to the temperature of the sky, the temperature of the surrounding earth/building surfaces, and again the view factor.

$$Q_{surf} = Q_{conv} + Q_{rad} = (h_{conv} * (T_{surf} - T_{amb}) + h_{rad} (T_{surf}{}^4 - T_{rad\_env}{}^4)) * S$$

Eq 3 Heat transfer in the internal surface of a wall

Where:

- Q_{surf} represents the overall surface heat transfer
- Q_{conv} represents the convective surface heat transfer

- Q_{rad} represents the radiant surface heat transfer
- h_{conv} represents the convective surface heat transfer coefficient
- h_{rad} represents the radiant surface heat transfer coefficient
- T_{surf} is the representative temperature of the surface
- T_{amb} is the representative temperature of the surrounding ambient air
- T_{rad_env} is the representative radiant temperature of the environment. For indoor cases it is obtained as a wheighted average of the surrounding surfaces
- S is the Surface area

The original heat transfer equation can be substituted by a linear form according to [18] , obtaining the following equation:

$$Q_{surf} = (h_{conv} * (T_{surf} - T_{amb}) + h_{rad}^{'} (T_{surf} - T_{rad\_env})) * S$$

Eq 4 Heat transfer in the internal surface of a wall with linearized convection

Where:

- $h_{rad}^{'}$ is the linearized radiant heat transfer coefficient

However, in the case of internal heat transfer, it was decided to join both heat transfer processes into one unique heat flux. This heat flux relative to the internal ambient temperature. It was considered that the simplification introduced through this approach was not very relevant in terms of model accuracy, as surface and ambient temperatures in this kind of test cells without windows were expected to be very similar.

$$Q_{surf} = h * (T_{surf} - T_{rad\_env}) * S$$

Eq 5 Heat transfer in the internal surface of a wall with linearized convection

Where:

- h is the overall heat transfer coefficient

The tested façade system does not comply with this assumption as it is more exposed to the external ambience and it is constructed with heavily inertial materials. However, this was not found problematic, as this system is part of the thermal model and not of its boundary conditions.

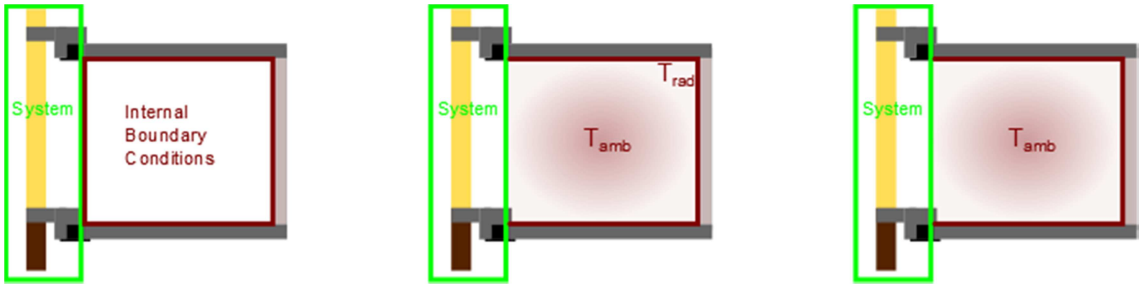

Fig 5 Left: Definition of internal boundary.

Center: Internal boundary conditions for segregated convective & radiative heat transfer.

Right: Internal boundary conditions for joint convective & radiative heat transfer.

The taken assumptions were verified with ambient & surface temperature data from the experimental campaign.

5. Identification of suitable places for sensor placement

5.1. Evaluation of the thermal field

The location of sensors requires of a careful study, to ensure that, once installed their signal will be accurate and representative of the measured variable. Within this study, a FDM analysis was performed in order to evaluate the expected thermal field in the thermal bridge area, and this information was used to select the most suitable places for the sensors.

Steady-state 2D thermal models of the three wall-slab junction details were made in order to find the most suitable places for sensor placement. The architectural details were modeled in TRISCO [19] and meshed according to [11] . Fig 6 shows the steady state result of one of the performed FDM analysis.

The selection of the location of sensors intended a balance between a reduced amount of sensors and the placement of sensors distributed across the architectural detail in order to provide sufficient data for the calibration of dynamic FDMs.

5.2. Feasibility of installation

Feasibility of the location was also evaluated, which was mainly related to weather-proofing. Sensors would have to be operative for several years. Outdoor locations with difficulties for sensors replacements had to ensure that sensors would not be damaged shortly after installation.

Due to weather-proof limitations, no heat flux meter was installed outdoors, and temperature sensors were embedded in concrete, which in turn provided more stable

temperature signals. Due to the stability of this solution, when possible, indoor temperature sensors were also embedded in concrete.

Furthermore, to avoid failure issues regarding failure of sensors in non-accessible locations, redundant sensors were located in external locations were replacement was estimated as difficultly achievable.

Due to the specific case of each of the slab-façade joints, not all internal locations where available in all joints:

- Floor 1: Only locations above the slab were possible
- Floor 2: All locations
- Roof: Only locations below the slab were possible

5.3. Selection of location

Suitability was defined with a series of specifications:

- Temperature sensors should be located at different isothermal zones, as they reflect areas differently influenced by internal or external boundary conditions in term of amplitude & phase-shift.
- Heat-flux sensors should be located at places with different heat flow densities.

Regarding the outer surface temperature, sensors were located in the centre of the slab. In this case, redundant sensors were placed.

Regarding internal temperature measurements, 2D steady-state models showed that the surface temperature of the concrete elements had a relevant gradient perpendicularly to the façade, and sensors where placed in the coldest & hottest places of the element:

- Locations above the concrete element:
    - Concrete-façade corner
    - Upper-inner corner of the concrete element

- Locations below the concrete elements:
    - Concrete-façade corner
    - Centre of the steel beam

Regarding heat flux measurements, most divergent heat flux densities were found above the slab. Furthermore, no locations were found below the slab, as the highly conductive surface of the steel beam and the reduced exposed area of the concrete element were evaluated unappropriated.

The selected locations where the following:

- Upper surface next to the façade. Even if in this area the heat flux was not one dimensional, this location was selected because of being the area with the highest heat flux.
- Centre of the internal vertical surface: This location was the only area where pseudo-1D surface heat flux was present.

These can be seen in Fig 6 .

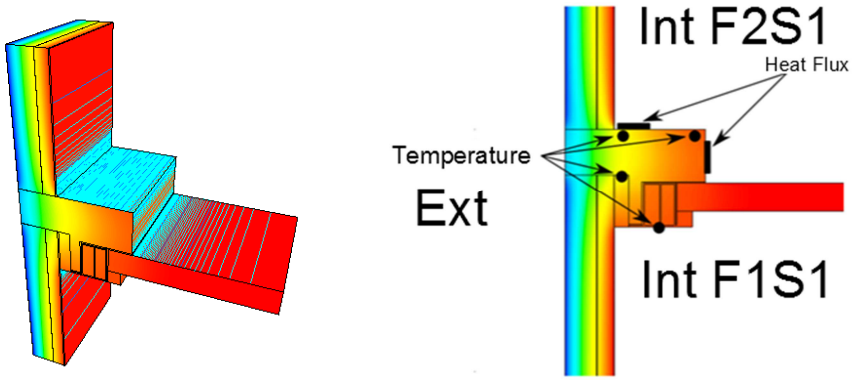

Fig 6 Thermal bridge on Floor 2 level: Steady-state model of (left). Internal sensor location (right)

The final sensor list and location can be found in Table 1.

Table 1. Sensor & location list

Beam Element	Type of measurement	Type of sensor	Format	Amount of sensors
Floor 1	Outdoor surface temperature	4-wire Pt100, 1/3 class B. Thermo Sensor	PVC Sealed for concrete-embedded applications.	2
	Indoor surface temperature			2
	Indoor heat flux	Heat flux tile. Phymeas.	Thickness: 1mm Size: 10cmx10cm	2
Floor 2	Outdoor surface temperature	4-wire Pt100, 1/3 class B. Thermo Sensor	PVC Sealed for concrete-embedded applications.	2
	Indoor surface temperature			4
	Indoor heat flux	Heat flux tile. Phymeas.	Thickness: 1mm Size: 10cmx10cm	2
Roof	Outdoor surface temperature	4-wire Pt100, 1/3 class B. Thermo Sensor	PVC Sealed for concrete-embedded applications.	2
	Indoor surface temperature			1

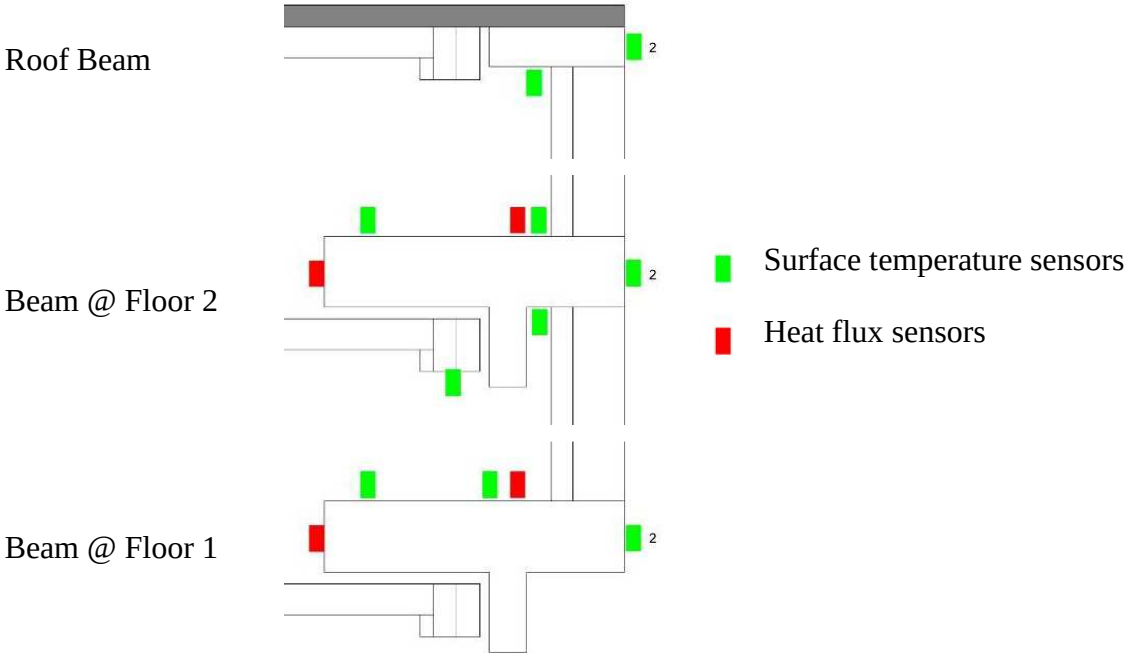

Fig 7 Location of sensors. Green: temperature. Red: Heat flux

6. Experimental campaign

The experimentation on the assessment of thermal bridges was conducted within the experimental campaign of the main project described in the integration frame. Depending on the experimental campaign, different façades were tested. Data provided in this paper was obtained during Phase 0 with the highly insulated sandwich façade construction.

In this campaign several temperature setpoint levels were established at each of the thermal zones. Data was divided in four datasets, which are indicated in Table 2.

Table 2. Experimental datasets for the highly insulated sandwich element

Dataset	Period	Outdoor conditions	Indoor Temperature	
			F1S1 (Floor 1)	F2S1 (Floor 2) + All neighbouring spaces in the building.
1	2012/I/19 – 2012/II/5	Winter period, average Temperature: 3-12 ºC	Constant, 29-31ºC	Constant, 29-31ºC
2	2012/II/6 – 2012/II/16	Winter period, average Temperature: 2-9 ºC	Constant, 20ºC	Constant, 20ºC
3	2012/II/17 – 2012/II/28	Winter period, average Temperature: 4-9 ºC	Highly variable, 20-30ºC	Nearly constant, 15-20ºC
4	2012/II/29 – 2012/III/11	Winter period, average Temperature: 6-12 ºC	Constant, 20ºC	Constant, 30ºC

1-minute raw experimental data was obtained from the experimental campaign and an hourly averaging process was conducted. As no data was missed in periods longer than 1h during the full experimental campaign, no data gaps needed to be solved. Daily average temperatures are shown in Fig 8 .

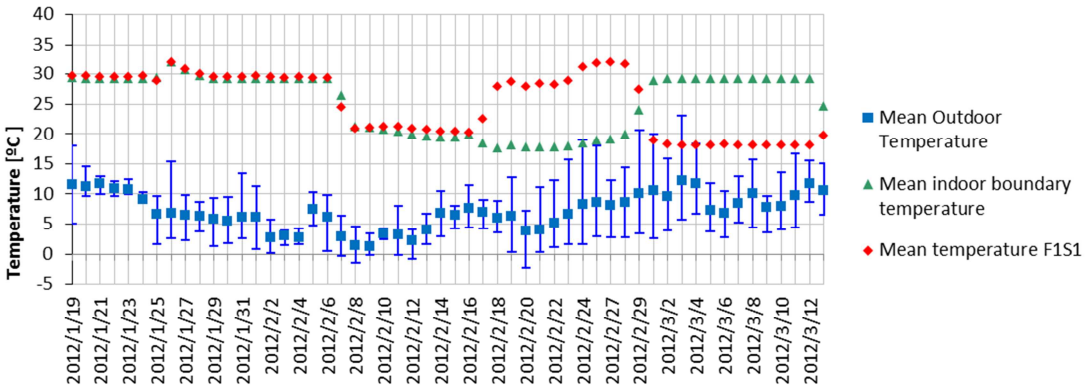

Fig 8 Daily average temperatures for the highly insulated sandwich element

During the design of the thermal bridge elements, attention was paid to minimizing 3D thermal bridging in corners and ensuring 2D heat transmission along the floor beams. This aim was verified by a thermographic study, which stated that, aside from 0.1-0.2m on each of the sides of the floor beams (which were 3,3m long), no 3D heat transmission processes were present in the floor beams, as a 2D thermal profile in the slab element is maintained in the full length of the element.

7. FDM modeling and calibration

The FDM modeling was conducted using VOLTRA [20] , a transient 2D-3D heat transfer modeling software. In this software, the architectural details were modeled in 2D and meshed according to [11] , and a parametric study was conducted to fix each of the thermal properties in the model. The calibrated parameters being the following:

- Surface heat transfer coefficients, h [W/m2K]
- Thermal capacity (Specific Heat * Density) of materials $c_p * \rho$ [kJ/m3K]
- Thermal conductivity of materials λ [W/mK]

During the construction process, strong efforts were made to ensure the quality of the test set up, and no uncertainty was expected in the dimensions and shape of the architectural detail.

The calibration process was conducted in steps:

0. An initial model was constructed by using thermal properties from the Phisibel database in VOLTRA [20] .
1. Thermal conductivity of materials was fixed by using Temperature data from nearly steady state periods.
2. Thermal capacity of materials was fixed by using Temperature data from transient periods.
3. Surface heat transfer coefficients were fixed by using heat flux data from steady state periods.

At each step the effect of the modification of the calibrated parameters in previously calibrated parameters was studied. Details range of estimation, and bibliographic references on the imposed thermal parameters, as well as the finally validated result can be found in sections 9.3 and 9.4.

The following results were obtained:

- Façade constructions: These elements were constructed with 30cm of insulating materials. The resulting very insulating (U<0.2 W/m2K) and almost massless elements required only a fine tuning of thermal conductivity values.
- Concrete elements: Floor slabs and thermal bridge elements required minor conductivity and capacity tuning, as the final values were similar to initial estimations and data from material catalogues.
- Heat transfer coefficients were found to be most difficult to calibrate. Different coefficients were required for upwards and downwards heat flow. Additionally reduced heat transfer coefficients were applied to corner areas.
- Dataset 3 presented highly unsteady conditions due to two situations. Firstly, as all the surrounding internal spaces where artificially cooled to generate a thermal gradient with the F1S1 room, as the heating system was found not able to meet the setpoint at all times. Additionally, when the setpoint was reached, a very strict deadband value produced short activation-deactivation osculation cycles of this system. Dataset 3 was not considered suitable for calibration due to a highly variable convection coefficient oscillation caused by:
    - The direction of the vertical convection was not always the same, as floor slabs were charged-discharged when indoor temperature oscilated.
    - The activation over short cycles of the fan coil heating system modified airflow around the indoor surface.

The final conclusion of this process is that material testing and precise construction of architectural details allows for a good control in heat transfer in solid materials, while convective processes need to be specifically verified prior to the estimation of the thermal behavior of a thermal bridge.

Instability of convective problems were mostly related to the HVAC system, which consisted on a fan-coil system located in the ceiling. The activation/deactivation cycles to keep setpoint temperatures in the test cells provided very different air velocities in the test cell. This problem should not be present, or at least be of lower relevance in test cells conditioned with different HVAC schemes.

Floor 1. Concrete beam, upper surface temperature. Indoors, next to the façade

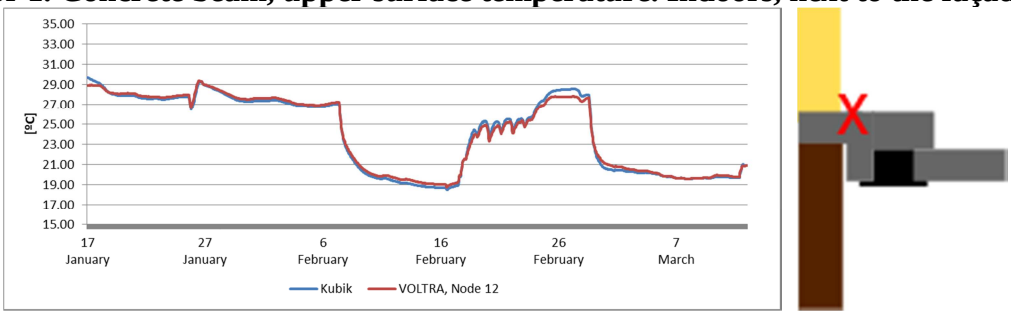

Floor 1. Concrete beam upper surface temperature. Indoors, opposite to the façade

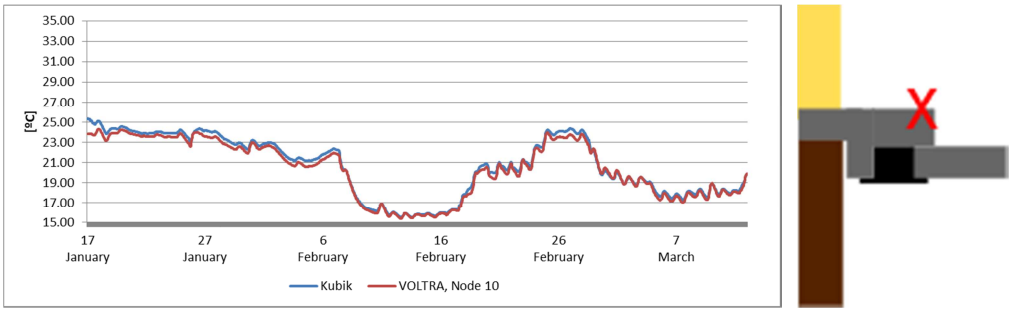

Floor 2. Concrete beam, lower surface temperature.

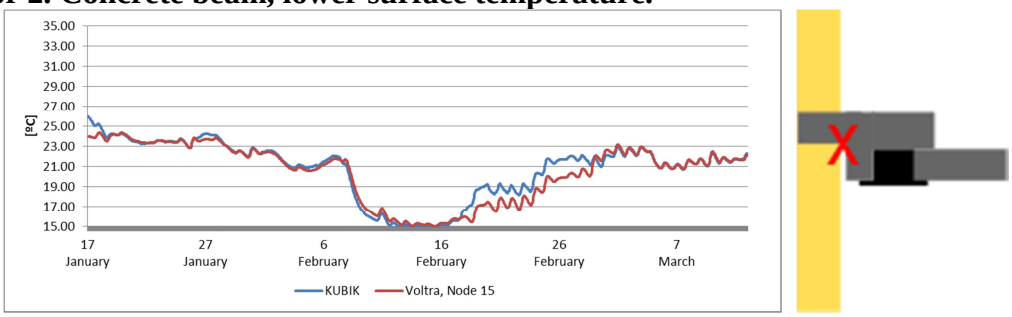

Floor 2. Concrete beam, Heat flux, indoors, next to the façade.

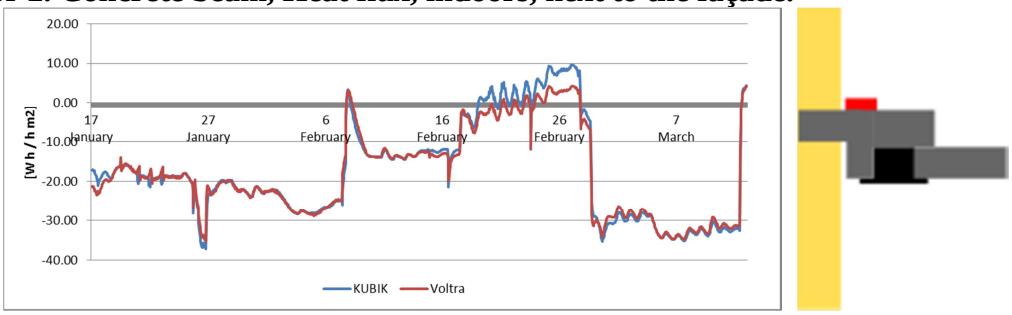

Note: The gap in the data series between FEB 17 and FEB 28, corresponds to Dataset 3, which is reported as non-acceptable in terms of model calibration, and is not ploted in this figure.

Fig 9 Comparison between experimental data and calibrated signals for selected temperature and heat flux signals.

8. Verification of the joint convection-radiation approach

Data from the experimental campaign was used to verify that temperature differences between surface and air temperature were sufficiently similar as to perform a joint modelling of convection and radiation processes in the internal side of the façade elements. As it can be seen in the Fig 10 , the difference between these temperatures was limited, except for those moments where heavy HVAC excitation was made, or where high temperature differences between test cells were present (Sequence 4).

Sequence 1

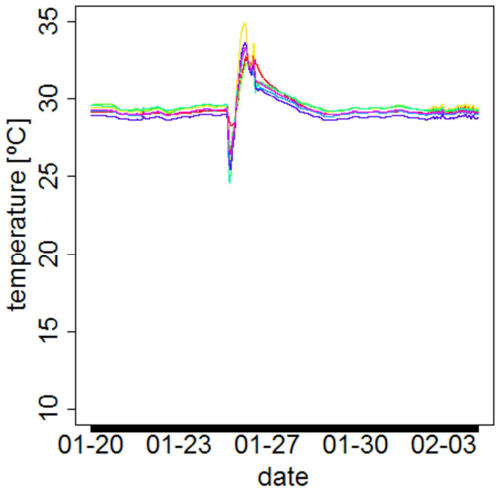

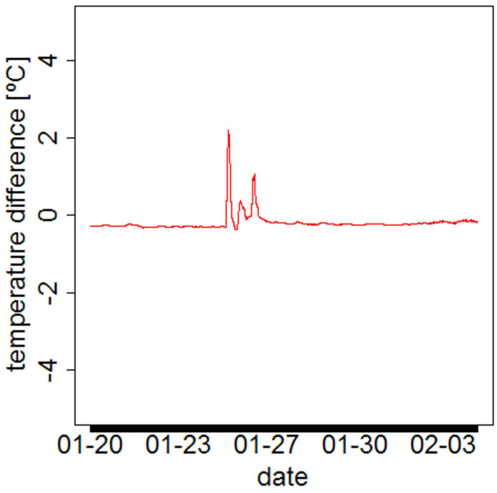

Sequence 2

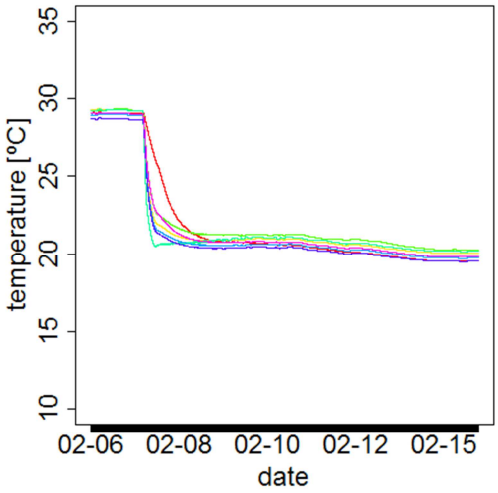

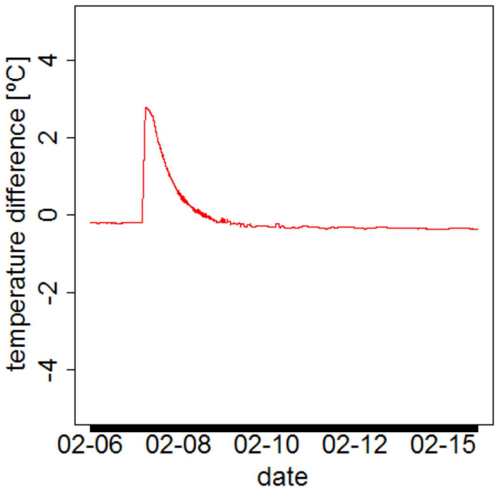

Sequence 3

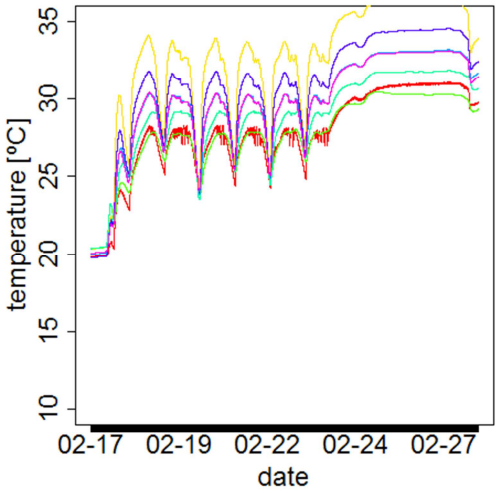

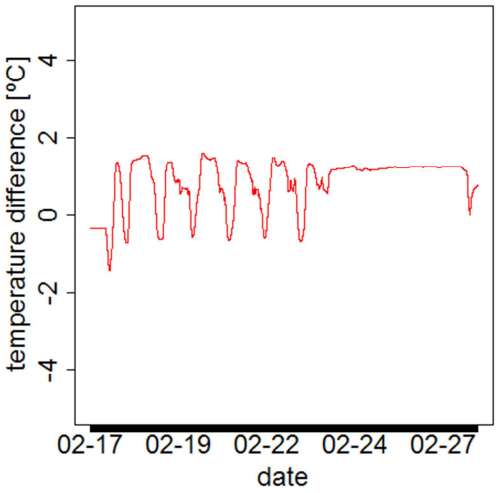

Sequence 4

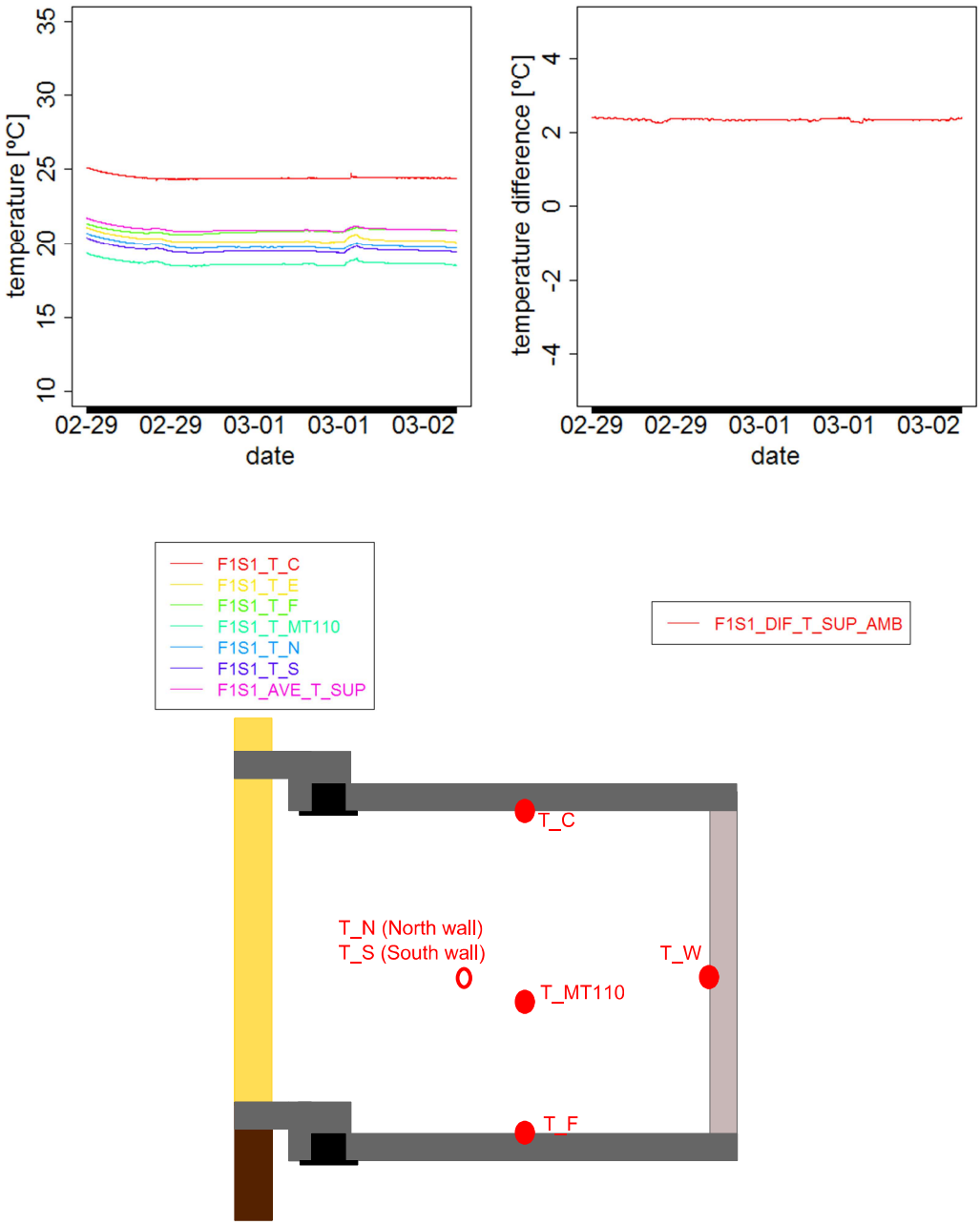

Fig 10 Surface, air and average temperatures (left)

maximum difference between individual signals to the average (right)

Location of sensors (Bottom)

The observed temperature differences were:

- Smaller than 0,5 ºC in steady states
- Around 1-3 ºC during the dynamic response when the HVAC system acts as full power.

- Stable at 2.2 ºC when a highly different temperature was present in a neighboring room. This situation was found specific to sequence 4, which is very specific to calibration purposes.

The observed differences due to highly HVAC fluctuating situations, and highly different surface temperatures due to opposed temperatures in neighboring test cells, were estimated specific to very seldom phenomena, and the inaccuracy introduced by the joint convection-radiation approach was assumed acceptable.

9. Modelling details of the FDM

9.1. Selected boundary conditions

The selected boundary conditions for each FDM account for the following:

- Outdoor: Surface temperature, measured at the concrete beam, average of signals (2-3 signals depending of the beam).
- Indoor: Indoor air temperature. Measured at three heights, 70, 110 and 170cm. The FDM uses the average of these three signals.

The selected boundary condition for the outdoor ambient was the surface temperature of the slab, as this temperature already accounted for the influence of solar radiation. This surface temperature was found very robust, as sensors placed in the same beam, produced nearly-identical signals. It is known that the surface temperature varies along the façade, as part of the 2-dimensional heat transfer phenomena, which is studied in this paper. However, when studying a case with highly insulated façade elements, it was found that although the considered boundary condition is not very representative of the surface temperature over the 1-dimensional areas, this did not produce significant differences in the surface temperature field inside the building.

9.2. Surface heat exchange model

The FDM was constructed based on the defined boundary conditions. In Fig 11 , an scheme of the surface heat transfer areas can be found. This heat exchange scheme was changed when an area with reduced heat transfer was required.

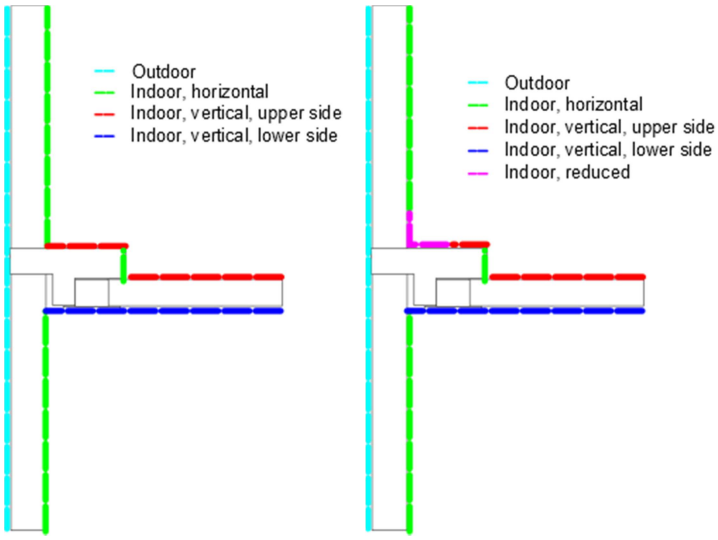

Fig 11 Surface Heat transfer scheme, initial approach(left) and modified approach with reduced heat transfer areas(right)

9.3. Material properties

Material properties were subjected to identification procedures. In Table 3, thermal parameters are provided. For each item, the range of estimation and a reference value from [21] are provided. Minimum and maximum values were established to the calibration of the parameters, based on experience of variation ranges for such elements. As it can be seen in this table, Insulation materials, and metal elements did not require of parameter estimation, and only concrete, which was not a standardized material supply for this experiment required parameter estimations.

Table 3. Parameters of the FDM, materials

Material	Parameter	Unit	Range			Calibrated
			Min	Max	Estimation CTE[21]	
Concrete	Thermal conductivity	W/mK	2	2,6	2,6	2,2
	Density	Kg/m3	2000	2400	2300	2300
	Heat capacity	kJ/kg	930			
Steel beam	Thermal conductivity	W/mK	50			
	Density	Kg/m3	7800			
	Heat capacity	kJ/kg	930			
Poliurethane	Thermal conductivity	W/mK	0,028			
	Density	Kg/m3	25			
	Heat capacity	kJ/kg	1470			
XPS	Thermal conductivity	W/mK	0,035			
	Density	Kg/m3	25			
	Heat capacity	kJ/kg	1470			

9.4. Surface heat transfer coefficients

The calibration of the thermal model required of a fine tuning of the surface heat transfer coefficients. This heat transfer accounted jointly for convection and radiation phenomena. Initially, all surfaces where considered with one heat transfer coefficient, but then reduced values were provided for corner areas, and different coefficients were identified for up and downwards heat flux periods. The reduced heat transfer in corner areas is estimated to be produced/required as the air velocity in these areas is reduced, when compared to more exposed areas. And the difference between upwards and downwards periods is an already known issue, which is even reflected in standardized heat transfer calculations [10] .

For each item, the range of estimation and a reference value from [10] are provided. Minimum and maximum values were established based on experience of variation ranges for such parameters.

Table 4. Parameters of the FDM, heat transfer coefficients

Item	Unit	Range			Calibrated
		Min	Max	Reference ISO [10]	
Inside, horizontal flux	W/m2K	3,5	7,7	7,7	4,0
Inside, horizontal flux, reduced	W/m2K	2	7,7	-	2,5
Inside, vertical, upward flux, Upper side	W/m2K	3,5	7,7	10	4,0
Inside, vertical, upward flux, Lower side	W/m2K	3,5	7,7	10	4,0
Inside, vertical, downward flux, Upper side	W/m2K	3,5	7,7	5,9	3,5
Inside, vertical, downward flux, Lower side	W/m2K	3,5	7,7	5,9	4,0
Inside, vertical, flux, reduced	W/m2K	3,5	7,7	-	3,5

10. Integration of the calibrated models into the main room model

The experimentation and calibration process which is described in this document was developed to produce a suitable thermal model of thermal bridges for its use in a thermal balance of a room.

From the calibrated model and according to the equation stated in section 3 (Integration Frame), the thermal influence of the thermal bridge was obtained. And used in the thermal balance of the room.

Aside from the previously used temperature and heat flux measurements, each model was defined to output dynamic inbound and outbound heat flow form the room. From the same model, the 1D heat transfer from façade and slab elements was calculated and applied to the corresponding surfaces. All additional heat was assigned to the "additional 2D heat transfer" term. Eq 6was applied (which is a reformulation of that previously stated in Eq 2)

$$Q_{2D} = Q_{Constructive\_detail} - Q_{1D}$$

Eq 6 Additional 2D heat transfer through thermal bridge

With the following Q_{1D} definition:

$$Q_{1D} = Q_{1D,Façade} * L_{Façade} + Q_{1D,Floor\_slab} * L_{Floor\_slab}$$

Where:

- All the heat transfer was referred to a reference room (F1S1 or F2S1 depending on the case), and heat flows were measured in the indoor surface/volume of this reference room.
- Q_{2D} was the additional heat transfer caused by the beam element
- $Q_{Constructive\_detail}$ was the heat gained/lost by the reference room
- Q_{1D} was the heat transferred through a 1D zone of the planar elements
- $Q_{1D,Façade}$ was the heat transferred through a 1D zone of the façade
- $Q_{1D,Floor\_slab}$ was the heat transferred through a 1D zone of the floor slab
- $L_{Façade}$ was the height of the façade modeled in the FDM model
- L_{Floor_slab} was the width of the floor slab modeled in the FDM model

Dimensions $L_{Façade}$ and L_{Floor_slab} were taken from the geometry modeled in Voltra, as shown in the following scheme:

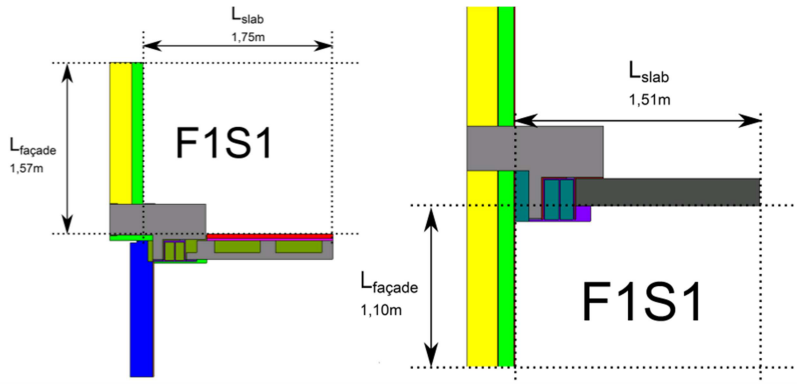

Fig 12 Sketch of the internal dimensions in the F1S1 room, in the FDM model for the beam-elements at floor 1 (left) and floor 2 (right) levels

All this process performed dynamically for each hourly timestep.

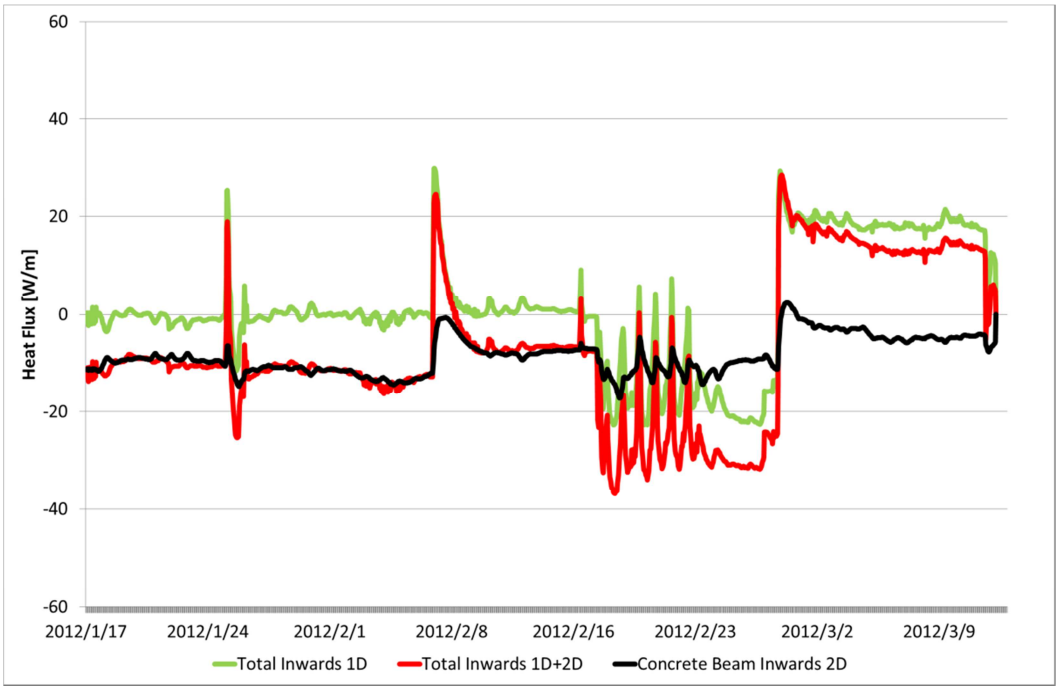

Fig 13 Concrete beam at floor 1 level. Hourly heat flows towards F1S1 zone in the modeled architectural detail.

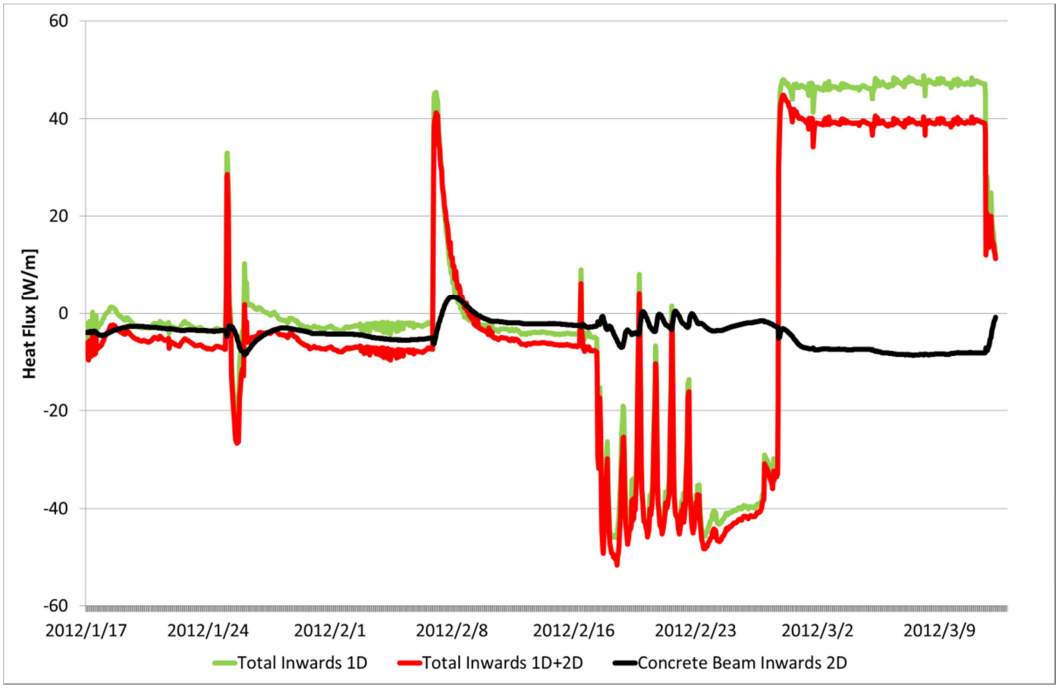

Fig 14 Concrete beam at floor 2 level. Hourly heat flows towards F1S1 zone in the modeled architectural detail.

The thermal influence of the concrete elements was found relevant, not only in terms of overall energy balance, but also in terms of short term response.

Depending on the boundary temperatures in each of the sequences, the additional heat transfer across the thermal bridge had different impact on the overall heat balance. In situations with small 1D heat transfer, heat transfer across concrete elements was far more relevant than 1D-heat transfer. This can be observed in situations such as sequences 1 & 2 of the concrete element at floor 1 level (Fig 13), where 1D heat transfer could even be neglected, during pseudo-steady-state periods. In situations with larger heat transfer situations, the concrete element provided 10-20% of surplus/reduced heat transfer over the analyzed junction detail.

It was also noticed that the time-response of the slab was far more slow than that of planar surfaces, as it was expected due to these elements being composed by bulk concrete, as opposed to insulation materials, void spaces,… on planar surfaces.

11. Summary and Conclusions

Within a research project with further objectives, the energy performance of thermal bridges generated in several concrete beam elements has been studied. This assessment was performed through a dynamic 2D thermal model, which was calibrated against experimental data. The thermal flow in these elements was found clearly bi-dimensional, which states the need of such analysis methods. Furthermore, not only the thermal field was calculated, but its results were reformulated to fit into the heat balance calculation of several rooms.

The models were found to be extremely sensible to surface convection and radiation heat transfer, while were reasonably stable to thermal properties of materials. The geometric description was considered exact as craftworks were supervised to avoid uncertainties of this kind. The sensitivity to surface heat transfer coefficients was mainly observed in heat flux signals, while temperature signals did not divert significantly with heat transfer coefficients similar to the finally calibrated one.

It was found extremely relevant to include heat transfer across these concrete elements for a proper heat balance analysis of the experiment. 2D heat flows were found very relevant in some cases where 1D heat transfer was very low or even neglectable. Even in situations with large 1-dimensional heat transfer, 2D heat flow accounted for modifications in the range of 10-20% for the analyzed junctions. It should be noted that 2D heat flow did not necessarily have the same direction to the 1D heat flow, so that it would be difficult to deal with it as a linear factor of 1D heat flows. The magnitude of this heat flux is found coherent with previous works on heat transfer such as [6] , where the influence of thermal bridges is estimated in 15%.

Within full scale testing of thermal performance of building elements with clearly non one-dimensional flow, it is considered that the use of methods such as the one exposed in this paper or others providing similar information is highly useful.

12. Acknowledgements

The authors would like to thank the Government of the Basque Country, who partially funded this work; and the University of Sevilla and Fraunhoffer IBP for their advice in the definition of the experimental set-up.

13. References

[1] U.S. Department of Energy (DOE), 2008 Buildings Energy Data Book, 2008.

[2] Pérez-Lombard L., et al, . A review on buildings energy consumption information, Energy and Buildings 40, 2008

[3] E.U., 2002/91/EC of the European Parliament and of the Council of 16th December 2002 on the Energy Performance of Buildings, 2002.

[4] E.U., 2010/31/EU of the European Parliament and of the Council, of 19 May 2010 on the Energy Performance of Buildings (recast), 2010.

[5] Clarke J.A. Energy simulation in building design. Butterworth-Heinemann, 2nd edition, Oxford (2001).

[6] ASIEPI, WP4, An effective Handling of Thermal Bridges in the EPBD Context - Final Report of the IEE ASIEPI Work on Thermal Bridges, http://www.asiepi.eu/ [2014/07/10]

[7] Tecnalia, "Kubik by Tecnalia", http://www.energiaenedificacion.com/kubik-by-tecnalia/ [2014/07/07]

[8] Tecnalia, "KUBIK by Tecnalia, Experimental Infrastructure for the Configuration of Zero Energy Buildings", http://www.tecnalia.com/en/sustainable-construction/infrastructure-a-equipment/infrastructure-a-equipment.htm, 2012.

[9] EN ISO 14683:1999. Thermal bridges in building construction. Linear thermal transmittance. Simplified methods and default values.

[10] EN ISO 6946: 2007. Building components and building elements – Thermal resistance and thermal transmittance – Calculation Method

[11] EN ISO 10211-1:1995. Thermal bridges in building construction. Calculation of heat flows and surface temperatures. Part I: General calculation methods.

[12] EN ISO 10211-2:2001. Thermal bridges in building construction. Calculation of heat flows and surface temperatures. Part II: Linear thermal bridges.

[13] García Gil, A., Modelado de Puentes Térmicos en la Simulación Térmica de Edificios, Departamento de Máquinas y Motores Térmicos ETSII, Universidad de Málaga, 2008.

[14] Martin K., Caracterización del comportamiento de los puentes térmicos en régimen estacionario y dinámico mediante ensayos y cálculo. Su influencia en la demanda energética de

edificios de viviendas. Department of Thermal Engineering, University of the Basque Country, Bilbao (2009).

[15] Martin, K. et al, Equivalent wall method for dynamic characterisation of thermal bridges, Energy And Buildings 55 (2012)

[16] Martin, K. et al, Methodology for the calculation of response factors through experimental tests and validation with simulation, Energy and Buildings 42 (2010)

[17] Martin, K et al, Problems In The Calculation Of Thermal Bridges In Dynamic Conditions, Energy and Buildings 43 (2011)

[18] Alvarez, S. Análisis Dinámico del Comportamiento Térmico de Edificios, Universidad de Sevilla (1986).

[19] TRISCO, computer program to calculate 3D & 2D steady state heat transfer in rectangular objects, version 12.0w, PHYSIBEL (2010)

[20] VOLTRA. Computer program to calculate 3D & 2D transient heat transfer in objects described in a rectangular grid using the energy balance technique, version 6.3w. Physibel, 2009

[21] IETcc, "CTE, Código Técnico de la Edificación", "Catálogo De Elementos Constructivos Del CTE", v6.3, March 2010.

[22] ASHRAE Handbook – Fundamentals ASHRAE (2001).

[23] Ben-Nakhi A.E. Adaptive construction modeling within whole building dynamic simulation. Department of Mechanical Engineering, University of Strathclyde, Glasgow (1995).

[24] Blanusa P. et Al., Comparison between ASHRAE and ISO thermal transmittance calculation methods, Energy and Buildings 39 (2007)

[25] Blomberg, T., Heat Conduction In Two And Three Dimensions. Computer Modeling of Building Physics Applications, Department of Building Physics, Lund University, Sweden (1996)

[26] Carpenter, S., Advances in modeling thermal bridges in building envelopes. Enermodal engineering limited, Kitchener (2001).

[27] Citterio M., M. Cocco and H. Erhorn-Kluttig. Thermal bridges in the EBPD context: overview on MS approaches in regulations. ASIEPI Information paper (2008).

[28] EN ISO 13786:2007. Thermal performance of building components. Dynamic thermal characteristics. Calculation methods.

[29] EN ISO 13789:1999. Thermal performance of buildings -- Transmission heat loss coefficient -- Calculation method.

[30] Karambakkam B K., A One-dimensional Approximation for Transient Multi-dimensional Conduction Heat Transfer in Building Envelopes. Oklahoma State University, School of Mechanical and Aerospace Engineering.

[31] Mao G., Dynamic calculation of thermal bridges, Energy and Buildings 26 (1997)

[32] Martin, K. et al, Analysis of a thermal bridge in a guarded hot box testing facility, Energy And Buildings 50 (2012)

[33] Strachan P, Simulation support for performance assessment of building components. Building and Environment 43 (2008)

[34] Strachan P, et al. Thermal Bridge Assessments, Energy Systems Research Unit, University of Strathclyde, Glasgow, Scotland

[35] Tadeau, A, et al. Simulation of dynamic linear thermal bridges using a boundary element method model in the frequency domain. Energy and Buildings 43 (2011)

[36] Theodosiou T.G. eta Al., The impact of thermal bridges on the energy demand of buildings with double brick wall constructions, Energy and Buildings, 40 (2008)

[37] Thorsell, T., Advances in Thermal Insulation. A computer program to query an atlas of building details (2002)

14. List of figures

15. List of tables